The 14th IFToMM World Congress, Taipei, Taiwan, October 25-30, 2015
DOI Number: 10.6567/IFToMM.14TH.WC.OS11.017

Hamiltonian Based Parallel Formulation for Open–loop Multibody System Dynamics

K. Chadaj* P. Malczyk† J. Frączek‡
Division of Theory of Machines and Robots
Institute of Aeronautics and Applied Mechanics
The Faculty of Power and Aeronautical Engineering
Warsaw University of Technology, Poland

Abstract—*The authors present a novel approach for the analysis of multibody system dynamics based on the Hamilton's equations of motion using joint canonical coordinates. The proposed Hamiltonian based divide and conquer formulation (HDCA) allows the use of massively parallel computing architectures due to the binary–tree structure of the algorithm. In this paper, only articulated, open–loop kinematic chains are taken into account. Joint velocities, joint momenta, and impulsive reaction loads at joints are efficiently computed with the use of HDCA algorithm. In this paper the HDCA formulation is applied for the dynamics simulation of open–loop chain involving 16 rigid bodies interconnected by revolute joints. The numerical results are compared to the outcome recorded by using acceleration based counterparts such as original Featherstone's DCA algorithm [1], and MSC.ADAMS commercial software.*

Keywords: Divide and Conquer, Hamilton's canonical equations, Multibody dynamics, Parallel algorithm

I. Introduction

There is a large variety of applications where the efficiency of the computations plays a crucial role. The group encompasses many systems including vehicles, biomechanical models, robots and multidisciplinary applications. Computations can be carried out by means of different types of formulations. To meet requirements for high–fidelity performance and accurate dynamics simulations of complex systems, it has become a practice to apply efficient, low order algorithms designed both for sequential and parallel computations. A lot of interest in developing efficient multibody dynamics algorithms manifests itself in myriad of formulations. Some researchers developed recursive order $O(n)$ formulations for dynamics simulations of multibody systems, e.g. [2], [3], [4], [5]. Recursive algorithms gave basis for further development of efficient low order formulations. As parallel computing resources became more available, researchers began to adapt the existing formulations or design completely new algorithms, suitable for parallel computing. Current parallel strategies are mainly based on the divide and conquer formulation developed by Featherstone [1] and continued by the others [6], [7], [8], [9]. Some of the parallelization strategies are even implemented in commercial multibody solvers [10]. Nevertheless, most of the formulations make use of acceleration–based equations of motion. On the other hand Hamilton's equations exhibit many advantageous features compared to their counterparts. To the best of authors' knowledge, it also appears that there is a lack of efficient and general formulations based on the Hamilton's approach.

In this paper we are trying to continue the research initiated in the other papers published recently by the authors [11], [12]. We propose a divide and conquer algorithm based on the Hamilton's canonical equations (HDCA) for handling dynamics of multibody systems with open–loops and tree–like topologies.

II. Algorithm formulation

In this section the parallel Hamiltonian based divide and conquer algorithm (HDCA) will be derived and explained. As the state of the system is described by means of joint coordinates and joint momenta, the entire formulation can be inherently divided into two steps. At first, joint velocities in conjunction with impulsive reaction forces are computed with divide and conquer assembly–disassembly scheme. Subsequently, the equations of motion are reformulated to evaluate the time derivatives of canonical momenta at joints. The entire algorithm exhibits logarithmic (linear) computational cost in case of parallel (sequential) implementation in terms of the number of bodies n in the system.

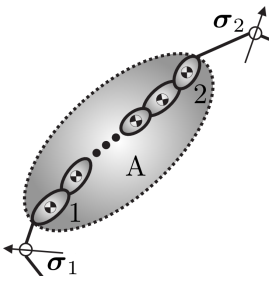

Fig. 1. A compound body with two handles

*kchadaj@meil.pw.edu.pl
†pmalczyk@meil.pw.edu.pl
‡jfraczek@meil.pw.edu.pl

A. Articulated momentum

Let consider a rigid body A connected with the rest of the system by kinematic joints (see Fig. 1). The specified point at which the body interacts with the preceding (predecessor) or the subsequent (successor) body via a kinematic joint is called a handle. The presence of the kinematic joint (and thus the handle as well) introduces additional dependencies on the momentum of the considered body. Let us define the articulated momentum vector of linear and angular momenta $\overline{\mathbf{P}} \in \mathcal{R}^6$ associated with the analyzed body at the handle location

$$\overline{\mathbf{P}} = \mathbf{D}\boldsymbol{\sigma} + \mathbf{H}\mathbf{p} \tag{1}$$

where the matrix $\mathbf{H} \in \mathcal{R}^{6\times n_f}$ represents the joint's motion subspace (n_f – degrees of freedom for the joint), whereas the matrix $\mathbf{D} \in \mathcal{R}^{6\times(6-n_f)}$ is associated with the subspace of constrained directions. The number of constraint equations imposed by the joint is $n_c = 6 - n_f$. The following condition holds $\mathbf{D}^T\mathbf{H} = \mathbf{0}$, which means that the mentioned subspaces are orthogonal to each other. Having joint canonical momenta $\mathbf{p}$ as the algorithm inputs, impulsive constraint loads $\boldsymbol{\sigma}$ are the unknowns to be calculated in the first phase of the HDCA algorithm.

For an exemplary body A with two handles at points O_1 and O_2, the momentum conservation principle can be formulated in the following manner

$$\mathbf{M}_1^A\mathbf{V}_1^A = \overline{\mathbf{P}_1^A} + \mathbf{S}_{12}^A\overline{\mathbf{P}_2^A} \tag{2}$$

$$\mathbf{M}_2^A\mathbf{V}_2^A = \mathbf{S}_{21}^A\overline{\mathbf{P}_1^A} + \overline{\mathbf{P}_2^A} \tag{3}$$

where $\mathbf{M}_1^A\mathbf{V}_1^A$ and $\mathbf{M}_2^A\mathbf{V}_2^A$ are the body's momentum vectors at specified locations, $\mathbf{M}_1^A \in \mathcal{R}^{6\times6}$, $\mathbf{M}_2^A \in \mathcal{R}^{6\times6}$ are generalized inertia matrices, vectors $\mathbf{V}_1^A \in \mathcal{R}^6$, $\mathbf{V}_2^A \in \mathcal{R}^6$ represents linear and angular velocities, and $\mathbf{S}_{12}^A$, $\mathbf{S}_{21}^A$ are shift matrices. The shift matrix provides a compact and simple form for transformations of spatial momentum, force and velocity vectors [13]. The combination of Eq. (1), and (2), (3) results in the following relation

$$\mathbf{V}_1^A = \boldsymbol{\xi}_{11}^A\mathbf{T}_1^A + \boldsymbol{\xi}_{12}^A\mathbf{T}_2^A + \boldsymbol{\xi}_{10}^A \tag{4}$$

$$\mathbf{V}_2^A = \boldsymbol{\xi}_{21}^A\mathbf{T}_1^A + \boldsymbol{\xi}_{22}^A\mathbf{T}_2^A + \boldsymbol{\xi}_{20}^A \tag{5}$$

which is the final form of the momentum conservation principle for a general body A with two handles. As the generalized mass matrices $\mathbf{M}_1^A$ and $\mathbf{M}_2^A$ are symmetric and positive definite, its inversions can be easily found.

B. Assembly

Equations (4) and (5) are the starting form for the assembly procedure in the HDCA algorithm. The assembly phase allows to determine all unknown absolute velocities $\mathbf{V}$, joint velocities $\dot{\mathbf{q}}$ and impulsive constraint forces $\mathbf{T}$ associated with the multibody system. Consider body A connected to body B by means of a general kinematic joint (see Fig. 2). The momentum conservation equations for A and B at handles 1 and 2 can be expressed as

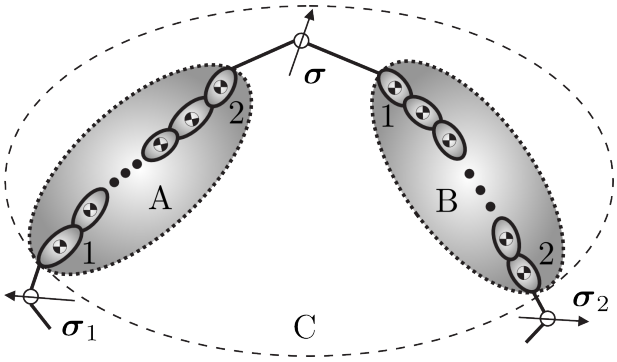

Fig. 2. The assembly of bodies A and B into body C

$$\mathbf{V}_1^A = \boldsymbol{\xi}_{11}^A\mathbf{T}_1^A + \boldsymbol{\xi}_{12}^A\mathbf{T}_2^A + \boldsymbol{\xi}_{10}^A \tag{6}$$

$$\mathbf{V}_2^A = \boldsymbol{\xi}_{21}^A\mathbf{T}_1^A + \boldsymbol{\xi}_{22}^A\mathbf{T}_2^A + \boldsymbol{\xi}_{20}^A \tag{7}$$

$$\mathbf{V}_1^B = \boldsymbol{\xi}_{11}^B\mathbf{T}_1^B + \boldsymbol{\xi}_{12}^B\mathbf{T}_2^B + \boldsymbol{\xi}_{10}^B \tag{8}$$

$$\mathbf{V}_2^B = \boldsymbol{\xi}_{21}^B\mathbf{T}_1^B + \boldsymbol{\xi}_{22}^B\mathbf{T}_2^B + \boldsymbol{\xi}_{20}^B \tag{9}$$

The interconnecting kinematic joint links the velocities of bodies A and B by means of the constraint equation in the form

$$\mathbf{V}_1^B - \mathbf{V}_2^A = \mathbf{H}\dot{\mathbf{q}} \tag{10}$$

Matrix $\mathbf{H}$ maps joint's velocity $\dot{\mathbf{q}}$ into the spatial velocity vector. To determine the interconnecting impulsive constraint force, equations (7) and (8) are substituted into Eq. (10), and then projected onto the subspace of constrained directions.

$$\mathbf{D}^T\left(\boldsymbol{\xi}_{11}^B\mathbf{T}_1^B + \boldsymbol{\xi}_{12}^B\mathbf{T}_2^B + \boldsymbol{\xi}_{10}^B\right) + - \mathbf{D}^T\left(\boldsymbol{\xi}_{21}^A\mathbf{T}_1^A + \boldsymbol{\xi}_{22}^A\mathbf{T}_2^A + \boldsymbol{\xi}_{20}^A\right) = \mathbf{0} \tag{11}$$

In accordance with the Newton's third law of motion, impulsive forces acting at the joint's handles satisfy the condition

$$\mathbf{T}_1^B = -\mathbf{T}_2^A = \mathbf{D}\boldsymbol{\sigma} \tag{12}$$

Combining equation (11) with (12), the expression for impulsive Lagrange multipliers $\boldsymbol{\sigma}$ can be found as a function of external impulsive forces $\mathbf{T}_\mathbf{1}^\mathbf{A}$ and $\mathbf{T}_\mathbf{2}^\mathbf{B}$

$$\boldsymbol{\sigma} = \mathbf{C}\mathbf{D}^T\left(\boldsymbol{\xi}_{12}^B\mathbf{T}_2^B - \boldsymbol{\xi}_{21}^A\mathbf{T}_1^A + \boldsymbol{\xi}_{10}^B - \boldsymbol{\xi}_{20}^A\right)$$

where

$$\mathbf{C} = -\left[\mathbf{D}^T\left(\boldsymbol{\xi}_{11}^B + \boldsymbol{\xi}_{22}^A\right)\mathbf{D}\right]^{-1}$$

There is no problem with the inversion as both matrices $\boldsymbol{\xi}_{11}^B$ and $\boldsymbol{\xi}_{22}^A$ are symmetric and positive definite. To simplify

the expression, let's define the following matrices

$$\mathbf{W} = \mathbf{D}\mathbf{C}\mathbf{D}^T \tag{13}$$

$$\boldsymbol{\beta} = \mathbf{D}\mathbf{C}\mathbf{D}^T \left(\boldsymbol{\xi}_{10}^B - \boldsymbol{\xi}_{20}^A\right) \tag{14}$$

Finally, the expression

$$\mathbf{T}_1^B = \mathbf{W}\boldsymbol{\xi}_{12}^B\mathbf{T}_2^B - \mathbf{W}\boldsymbol{\xi}_{21}^A\mathbf{T}_1^A + \boldsymbol{\beta} \tag{15}$$

describes how the impulsive interconnecting force depends on the impulsive forces at the boundaries.

Let us define the articulated body C as an assembly of bodies A and, B through the interconnecting joint. The handles at points O_1 and O_2 for body C are coincident with external handles O_1 for body A, and O_2 for body B, and results in the following relations

$$\mathbf{V}_1^C = \mathbf{V}_1^A \quad \text{and} \quad \mathbf{T}_1^C = \mathbf{T}_1^A \tag{16}$$

$$\mathbf{V}_2^C = \mathbf{V}_2^B \quad \text{and} \quad \mathbf{T}_2^C = \mathbf{T}_2^B \tag{17}$$

To determine analogous momentum conservation equations for articulated body C, equation (15) needs to be substituted into equations (6) and (9) to give

$$\mathbf{V}_1^C = \boldsymbol{\xi}_{11}^C\mathbf{T}_1^C + \boldsymbol{\xi}_{12}^C\mathbf{T}_2^C + \boldsymbol{\xi}_{10}^C \tag{18}$$

$$\mathbf{V}_2^C = \boldsymbol{\xi}_{21}^C\mathbf{T}_1^C + \boldsymbol{\xi}_{22}^C\mathbf{T}_2^C + \boldsymbol{\xi}_{20}^C \tag{19}$$

where the coefficients are expressed as

$$\boldsymbol{\xi}_{11}^C = \boldsymbol{\xi}_{11}^A + \boldsymbol{\xi}_{12}^A\mathbf{W}\boldsymbol{\xi}_{21}^A \tag{20}$$

$$\boldsymbol{\xi}_{12}^C = -\boldsymbol{\xi}_{12}^A\mathbf{W}\boldsymbol{\xi}_{12}^B \tag{21}$$

$$\boldsymbol{\xi}_{21}^C = -\boldsymbol{\xi}_{21}^B\mathbf{W}\boldsymbol{\xi}_{21}^A = \left(\boldsymbol{\xi}_{12}^C\right)^T \tag{22}$$

$$\boldsymbol{\xi}_{22}^C = \boldsymbol{\xi}_{22}^B + \boldsymbol{\xi}_{21}^B\mathbf{W}\boldsymbol{\xi}_{12}^B \tag{23}$$

$$\boldsymbol{\xi}_{10}^C = \boldsymbol{\xi}_{10}^A - \boldsymbol{\xi}_{12}^A\boldsymbol{\beta} \tag{24}$$

$$\boldsymbol{\xi}_{20}^C = \boldsymbol{\xi}_{20}^B + \boldsymbol{\xi}_{21}^B\boldsymbol{\beta} \tag{25}$$

The equations (20)–(25) are the main formulas for the HDCA algorithm and allow to assembly articulated body C in terms of bodies A and B. At this step it is possible to perform the hierarchic assembly process for the entire system based on the binary tree associated with the topology of the system (see Fig. 3). The phase finishes when the root node, which connects the articulated body to the mechanism's base, is reached. At this point, the boundary conditions can be applied.

C. Boundary conditions

Let's define the resulting equations for the whole system in the form of equations (18)–(19). In the case of the unbranched kinematic chains, equation (18) refers to the tip of the chain. Thus, the impulsive constraint force $\mathbf{T}_2^C$ is known to be zero. This fact implies that Eq. (18) simplifies to

$$\mathbf{V}_1^C = \boldsymbol{\xi}_{11}^C\mathbf{T}_1^C + \boldsymbol{\xi}_{10}^C \tag{26}$$

where the expressions

$$\mathbf{T}_1^C = \mathbf{D}_1\boldsymbol{\sigma}_1 \tag{27}$$

$$\mathbf{V}_1^C = \mathbf{H}_1\dot{\mathbf{q}}_1 \tag{28}$$

relate to the first kinematic joint connecting the chain to the fixed base. Projection of the Eq. (26) onto the subspace of constrained directions $\mathbf{D}_1$, and the application of Eq. (27) allow to determine the unknown impulsive Lagrange multipliers $\boldsymbol{\sigma}_1$ as

$$\boldsymbol{\sigma}_1 = -\left(\mathbf{D}_1^T\boldsymbol{\xi}_{11}^C\mathbf{D}_1\right)^{-1}\mathbf{D}_1^T\boldsymbol{\xi}_{10}^C = \mathbf{C}_1\mathbf{D}_1^T\boldsymbol{\xi}_{10}^C \tag{29}$$

Once more, there is no problem with the inversion as the matrix $\boldsymbol{\xi}_{11}^C$ remains symmetric and positive definite. At this point, the absolute velocity $\mathbf{V}_1^C$ can be computed with use of Eq. (26). Projection of Eq. (28) onto the joint's motion subspace $\mathbf{H}_1$ results in the joint velocity $\dot{\mathbf{q}}_1$

$$\dot{\mathbf{q}}_1 = \mathbf{H}_1^T\mathbf{H}_1\dot{\mathbf{q}}_1 = \mathbf{H}_1^T\mathbf{V}_1^C \tag{30}$$

where $\mathbf{H}_1^T\mathbf{H}_1 = \mathbf{I}$ is the identity matrix.

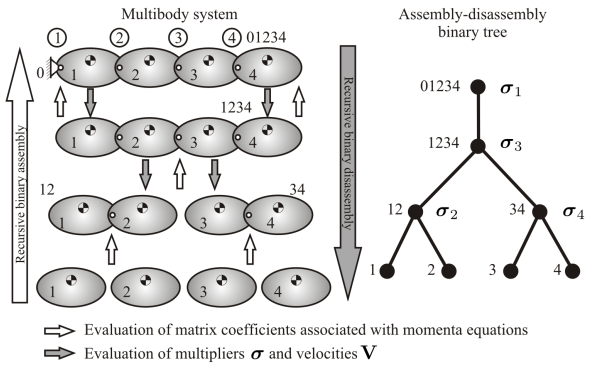

Fig. 3. Assembly–disassembly process for multibody system

D. Disassembly phase

The disassembly phase begins when the boundary impulsive constraint forces $\mathbf{T}_1^C$ and $\mathbf{T}_2^C$ from the previous paragraph are computed. These values are passed to the proceeding computational nodes (i.e. leafs of the binary tree) as indiciated in Fig. 3. With the use of the momentum conservation equations (6)–(9), handles coincidence conditions (16)–(17) and impulsive force relations (Eq. (15)), it is possible to determine impulsive constraint forces and absolute velocities for all bodies in the system in the disassembly phase. Subsequently, equation (10), when projected onto the corresponding joint's motion subspace, allows the calculation of joint velocities for all kinematic joints in the system.

E. Accumulated momenta

Let us start our further considerations by writing the equations of motion of a body in terms of absolute momenta at arbitrary point O (cf. [4], [13])

$$\dot{\mathbf{P}}_O + \dot{\mathbf{S}}_O \mathbf{P}_O = \mathbf{Q}_O \tag{31}$$

where

$$\dot{\mathbf{S}}_O = \begin{bmatrix} \mathbf{0} & \mathbf{0} \\ \mathbf{v}_O & \mathbf{0} \end{bmatrix}_{6x6} \tag{32}$$

$\mathbf{v}_O$ is the translational velocity vector with respect to the global reference frame, $\mathbf{Q}_O$ is a vector of spatial external loads acting on the body at point O, and $\mathbf{P}_O$ is a spatial momentum vector associated with the body at point O. Similarly as in the previous section, let us consider body A connected to the body B by means of a general kinematic joint (see Fig. 2). Moreover, let us assume that both bodies have two consecutively numbered handles, by which they are connected with the predecessor and successor. The equations of motion for body A and body B are as follows:

$$\dot{\mathbf{P}}_1^A + \dot{\mathbf{S}}_1^A \mathbf{P}_1^A = \mathbf{Q}_1^A + \mathbf{F}_1^A + \mathbf{S}_{12}^A \mathbf{F}_2^A \tag{33}$$

$$\dot{\mathbf{P}}_1^B + \dot{\mathbf{S}}_1^B \mathbf{P}_1^B = \mathbf{Q}_1^B + \mathbf{F}_1^B + \mathbf{S}_{12}^B \mathbf{F}_2^B \tag{34}$$

In accordance with the Newton's laws, the spatial (and unknown) reaction forces $\mathbf{F}$ have to satisfy the condition

$$\mathbf{F}_1^B = -\mathbf{F}_2^A \tag{35}$$

This in turn allows to substitute the force $\mathbf{F}_1^B$ from the Eq. (34) into Eq. (33). The resulting equations of motion of the compound body A–B are as follows

$$\begin{aligned} \dot{\mathbf{P}}_1^A + \mathbf{S}_{12}^A \dot{\mathbf{P}}_1^B + \dot{\mathbf{S}}_1^A \mathbf{P}_1^A + \dot{\mathbf{S}}_1^B \mathbf{P}_1^B = \\ = \mathbf{Q}_1^A + \mathbf{S}_{12}^A \mathbf{Q}_1^B + \mathbf{F}_1^A + \mathbf{S}_{12}^A \mathbf{S}_{12}^B \mathbf{F}_2^B \end{aligned} \tag{36}$$

Noticing that $\dot{\mathbf{S}}_1^B = \dot{\mathbf{S}}_1^A + \dot{\mathbf{S}}^A$, the above equation can be rearranged to more convenient form

$$\begin{aligned} \frac{d}{dt}\left(\mathbf{P}_1^A + \mathbf{S}_{12}^A \mathbf{P}_1^B\right) + \dot{\mathbf{S}}_1^A \left(\mathbf{P}_1^A + \mathbf{S}_{12}^A \mathbf{P}_1^B\right) = \\ = \left(\mathbf{Q}_1^A + \mathbf{S}_{12}^A \mathbf{Q}_1^B\right) + \mathbf{F}_1^A + \mathbf{S}_{12}^A \mathbf{S}_{12}^B \mathbf{F}_2^B \end{aligned} \tag{37}$$

After the substitutions, equation (37) becomes the equation of motion for the compound body C composed of bodies A, and B,

$$\dot{\mathbf{P}}_1^C + \dot{\mathbf{S}}_1^C \mathbf{P}_1^C = \mathbf{Q}_1^C + \mathbf{F}_1^C + \mathbf{S}_{12}^C \mathbf{F}_2^C \tag{38}$$

where $\mathbf{P}_1^C$ and $\mathbf{Q}_1^C$ are accumulated momenta and accumulated external loads. At this point it is possible to perform the hierarchic assembly process for the whole system based on the binary tree decomposition. The phase finishes when the root node, which connects the articulated body to the mechanism's base body, is reached.

F. Derivatives of canonical momenta

Let us now assume, that body C represents the whole considered system. The projection of the equation (38) onto the first joint's motion subspace allows to compute the time derivatives of the first joint canonical momenta

$$\dot{\mathbf{p}}_1 = \mathbf{H}_1^T \left(\mathbf{Q}_1^C - \dot{\mathbf{S}}_1^C \mathbf{P}_1^C\right) + \dot{\mathbf{H}}_1^T \mathbf{P}_1^C \tag{39}$$

The constraint force $\mathbf{F}_2^C$ is zero as it refers to the free tip of the open–loop chain, whereas the constraint force $\mathbf{F}_1^C$ is canceled due to the projection onto the appropriate joint motion subspace. On the other hand, the comparison of the accumulated momenta definition (Eq. (1)) with the momentum conservation principle (Eq. (2)–(3)) reveals the fact, that there is a clear dependency between the accumulated and the articulated momenta

$$\begin{aligned} \mathbf{P}_1^A + \mathbf{S}_{12}^A \mathbf{P}_1^B = \mathbf{P}_1^C = \overline{\mathbf{P}_1^C} + \mathbf{S}_{12}^C \overline{\mathbf{P}_2^C} = \\ = \left(\overline{\mathbf{P}_1^A} + \mathbf{S}_{12}^A \overline{\mathbf{P}_2^A}\right) + \mathbf{S}_{12}^A \left(\overline{\mathbf{P}_1^B} + \mathbf{S}_{12}^B \overline{\mathbf{P}_2^B}\right) \end{aligned} \tag{40}$$

Because $\mathbf{P}_1^B = -\mathbf{P}_2^A$ (compare with Eq. (12)) and the system is a open loop kinematic chain, the expression simplifies to

$$\mathbf{P}_1^C = \overline{\mathbf{P}_1^A} \tag{41}$$

As all articulated momenta (including $\overline{\mathbf{P}_1^A}$) are already known, there is no need to compute any accumulated momenta vectors.

The analogous process compared to that presented above can be carried out for articulated external loads. This time, the accumulated external loads have to be computed as

$$\mathbf{Q}_1^A = \overline{\mathbf{Q}_1^A} + \mathbf{S}_{12}^A \overline{\mathbf{Q}_2^A} \tag{42}$$

$$\mathbf{Q}_1^B = \overline{\mathbf{Q}_1^B} + \mathbf{S}_{12}^B \overline{\mathbf{Q}_2^B} \tag{43}$$

Based on the divide and conquer algorithm, it is possible to develop an assembly–disassembly procedure for calculating external and accumulated loads, which exhibits logarithmic computational cost in parallel.

$$\mathbf{Q}_1^C = \mathbf{Q}_1^A + \mathbf{S}_{12}^A \mathbf{Q}_1^B = \overline{\mathbf{Q}_1^A} \tag{44}$$

If the external loads do not depend on the velocity terms, they can be computed during the evaluation of joint velocities. Otherwise, the external loads have to be rearranged in terms of momenta (instead of velocities). With all velocity terms, articulated momenta and external loads known, the derivative of any canonical momenta k (related to body K) can be computed as

$$\dot{\mathbf{p}}_k = \mathbf{H}_k^T \left(\overline{\mathbf{Q}_1^K} - \dot{\mathbf{S}}_1^K \overline{\mathbf{P}_1^K}\right) + \dot{\mathbf{H}}_{k1}^T \overline{\mathbf{P}_1^K} \tag{45}$$

The above equations (45) for time derivatives of joint momenta together with joint velocities constitute the set of $2n$ (n – number of joints) Hamilton's canonical equations that need to be integrated to obtain the state of the system in the next time instant.

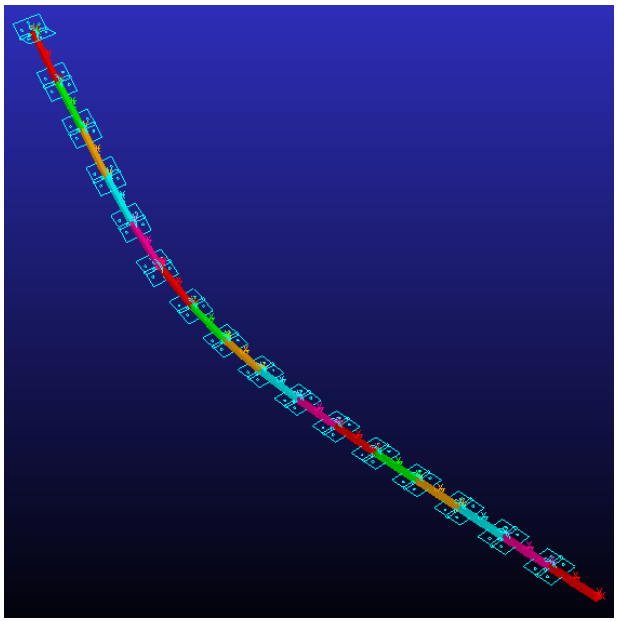

Fig. 4. The pendulum with 16 rigid bodies

III. Numerical test case

This section presents the results of numerical test cases performed to demonstrate the correctness of the methodology described above. The outcomes are compared against the commercial MSC.Adams software (RKF45 integration procedure) and Featherstone's acceleration based formulation (DCA) [1] implemented in MATLAB (ode45 integration procedure). Absolute and relative tolerances of the integrators are set to 10^{-6}. An unbranched pendulum consisting of 16 rigid bodies is taken into account (see Fig. 4). The bodies are interconnected by revolute joints. Each body has the characteristic length $l = 1m$, the mass $m = 1kg$ and inertia $J = diag\left(\begin{bmatrix}1 & 1 & 1\end{bmatrix}\right) kgm^2$ about the local coordinate frame associated with the body. Initially, the pendulum was positioned horizontally with all joint velocities equal to zero.

The numerical experiments allow to confirm the exactness of the HDCA algorithm for multibody systems consisting of open kinematic loops. Figure 5 presents the conservation of the total energy for 10 seconds of the simulation time. For all cases the value of the total energy remains constant and consistent with Featherstone's DCA approach, and the outcome from MSC.Adams commercial software. Kinetic and potential energy agree as well. Figure 6 directly compares the conservation of the total energy between HDCA and DCA algorithms. Figures 7 and 8 show the position and the translational velocity of the end point of the 16–body chain. As it is shown in the graphs, the HDCA algorithm preserves the correct motion of the tip for longer simulation times without any additional constraints stabilization methods involved in the solution process, and despite the fact of high–speed, high–frequency unpredictable changes in the motion of the system. During the 10 seconds of the simulation time, the integration of the equations using non-stiff routine took 67.3 seconds of real time for DCA and 60.9 seconds for HDCA for the similar, serial implementation in MATLAB. The DCA algorithm had to invoke the the right hand side function 3493 times, while the number of function evaluations for the HDCA algorithm was less and amounted to 3169 times.

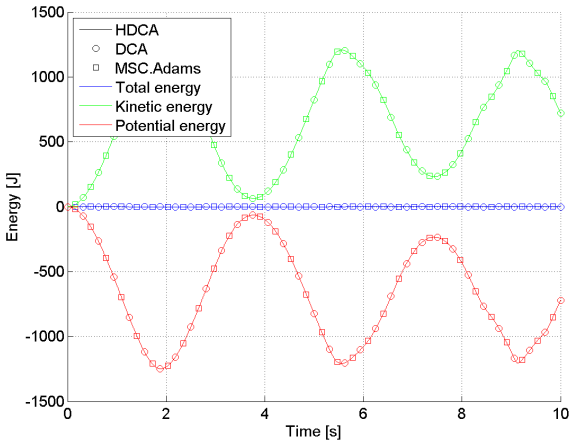

Fig. 5. The total, kinetic and potential energy of the chain

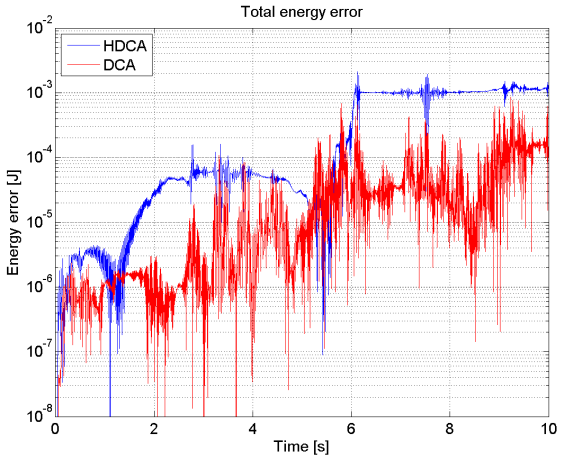

Fig. 6. The comparison of the total energy error

IV. Conclusions

The formulation presented in the paper describes the novel HDCA algorithm, which takes the advantages of the Hamilton's canonical equations and inherently the recursive divide and conquer scheme. The method can fairly easily be programmed in parallel achieving logarithmic $O(\log_2 n)$ computational cost for n threads, while sequentially the cost remains linear $O(n)$. The number of state variables

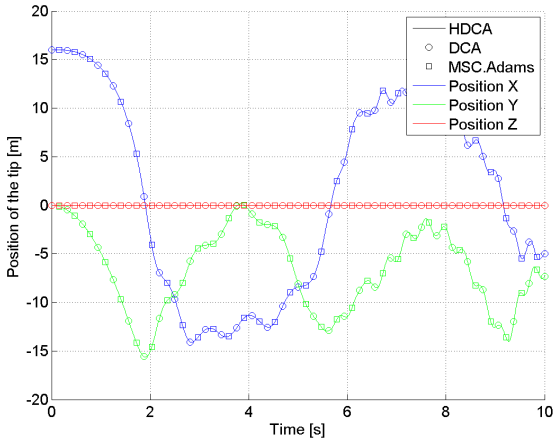

Fig. 7. The X, Y and Z coordinate position of the tip of the chain

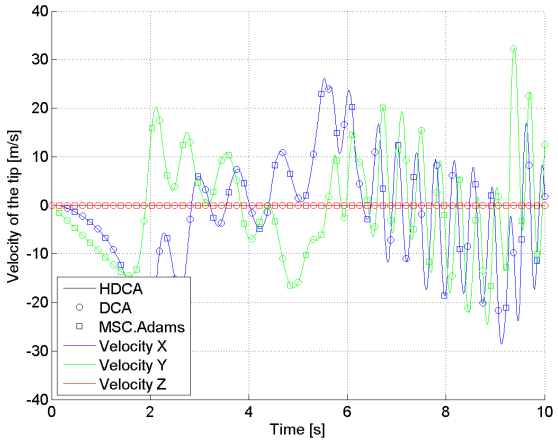

Fig. 8. The X, Y and Z coordinate velocity of the tip of the chain

required for forward dynamics analysis is reduced to minimum through the use of joint coordinates, which facilitate the solution of the equations of motion. The numerical test case presented in the paper indicates that the HDCA approach is slightly faster than the analogous implementation of the DCA algorithm and is numerically stable in terms of the total energy conservation. This qualifies the HDCA method for the study of more complex applications, where the usage of classical approaches would be potentially troublesome due to the adverse task conditioning. It is worth noticing that the presented method does not require the computation of the system's Hamiltonian nor its partial derivatives. On the other hand, the literature shows [14], [15], that the Hamilton's formalism exhibits a predominance over the Newton-Euler's equations of motion in terms of accuracy and constraint fulfillment. These benefits should be taken into consideration in further development of the algorithm for closed-loop topologies.

V. Acknowledgments

This work has been supported by the National Science Centre under grant no. DEC–2012/07/B/ST8/03993.

References

[1] R. Featherstone, "A divide-and-conquer articulated body algorithm for parallel O(log n) calculation of rigid body dynamics. Part 1: Basic algorithm," *International Journal of Robotics Research*, vol. 18, pp. 867–875, 1999.

[2] R. Featherstone, "The calculation of robot dynamics using articulated-body inertias," *International Journal of Robotics Research*, vol. 2, pp. 13–30, 1983.

[3] D. S. Bae and E. J. Haug, "A recursive formulation for constrained mechanical system dynamics: Part I: Open loop systems," *Mechanics of Structures and Machines*, vol. 15, pp. 359–382, 1987.

[4] J. Naudet, D. Lefeber, F. Daerden, and Z. Terze, "Forward dynamics of open-loop multibody mechanisms using an efficient recursive algorithm based on canonical momenta," *Multibody System Dynamics*, vol. 10(1), pp. 45–59, 2003.

[5] P. Malczyk and J. Frączek, "Cluster computing of mechanisms dynamics using recursive formulation," *Multibody System Dynamics*, vol. 20(2), pp. 177–196, 2008.

[6] R. Mukherjee and K. Anderson, "A logarithmic complexity divide-and-conquer algorithm for multi-flexible articulated body systems," *Journal of Computational and Nonlinear Dynamics*, vol. 2(1), pp. 10–21, 2007.

[7] P. Malczyk and J. Frączek, "A divide and conquer algorithm for constrained multibody system dynamics based on augmented lagrangian method with projections-based error correction," *Nonlinear Dynamics*, vol. 70(1), 2012.

[8] M. Poursina and K. Anderson, "An extended divide-and-conquer algorithm for a generalized class of multibody constraints," *Multibody System Dynamics*, vol. 29(3), pp. 235–254, 2013.

[9] R. Mukherjee and P. Malczyk, "Efficient approach for constraint enforcement in constrained multibody system dynamics," in *In Proc. of the ASME 2013 IDETC/CIE Conf. on Multibody Systems, Nonlinear Dynamics, and Control, Portland, USA*, 2013.

[10] P. Malczyk and J. Frączek, "Evaluation of parallel efficiency in modeling of mechanisms using commercial multibody solvers," *The Archive of Mechanical Engineering*, vol. LVI(3), pp. 237–249, 2009.

[11] P. Malczyk, K. Chadaj, and J. Frączek, "Efficient formulation for open loop multibody system dynamics based on hamilton's canonical equations," in *Proceedings of the 12th CONFERENCE on Dynamical Systems - Theory and Applications*, (Łódź, Poland), December 2-5 2013.

[12] P. Malczyk, J. Frączek, and K. Chadaj, "A parallel algorithm for multi-rigid body system dynamics based on the hamilton's canonical equations," in *Proceedings of the 3rd Joint International Conference on Multibody System Dynamics The 7th Asian Conference on Multibody Dynamics*, (Busan, Korea), June 30-July 3 2014.

[13] A. Jain, "Unified formulation of dynamics for serial rigid multibody systems," *Journal of Guidance, Control, and Dynamics*, vol. 14, pp. 531–542, 1991.

[14] E. Bayo and A. Avello, "Singularity free augmented Lagrangian algorithms for constrained multibody dynamics," *Nonlinear Dynamics*, vol. 5, pp. 247–255, 1994.

[15] H. Lankarani and P. Nikravesh, "Application of the canonical equations of motion in problems of constrained multibody systems with intermittent motion," *Advances in Design Automation*, vol. 1, pp. 417–423, 1988.